Glycinamide, a glycine precursor, caught in the gas phase: a laser-ablation jet-cooled rotational study

E. R. Alonso,[1] L. Kolesniková,[1] E. Białkowska-Jaworska,[2] Z. Kisiel,[2] I. León,[1] J.-C. Guillemin,[3] and J. L. Alonso[1]

[1]*Grupo de Espectroscopia Molecular (GEM), Edificio Quifima, Área de Química-Física*
Laboratorios de Espectroscopia y Bioespectroscopia, Parque Científico UVa, Unidad Asociada CSIC,
47011 Valladolid, Spain
[2]*Laboratory of Mm- and Submm- Spectroscopy, Institute of Physics, Polish Academy of Sciences*
Al. Lotników 32/46
02668 Warszawa, Poland
[3]*Institut des Sciences Chimiques de Rennes, École Nationale Supérieure de Chimie de Rennes, CNRS, UMR 6226,*
Laboratorios de Espectroscopia y Bioespectroscopia, Parque Científico UVa, Unidad Asociada CSIC,
11 Allée de Beaulieu, CS 50837, 35708 Rennes Cedex 7, France

Abstract

Glycinamide, a glycine precursor, has been successfully generated in the gas phase by laser ablation of its hydrochloride salt, and its microwave spectrum is reported for the first time. The existence of a single structure stabilized by a N_a–H $\cdots$ $N_t H_2$ hydrogen bond has been revealed in supersonic expansion by broadband Fourier transform microwave spectroscopy. The complex nuclear quadrupole coupling hyperfine structure due to the two ^{14}N nuclei has been completely resolved and analyzed. The first precise data obtained on this glycine precursor could be of great importance for possible future identifications in the interstellar medium.

Keywords: catalogs — ISM: molecules — molecular data — techniques: spectroscopic

1. INTRODUCTION

The detection of glycine in the interstellar medium (ISM) is one of the most pursued targets for the researchers in astrochemistry and astrophysics. Its presence would confirm that complex chemical reactions in this medium can synthesize the fundamental building blocks of life and thus, that its presence in the Universe may be more widespread than accepted (Kwok 2011; Guillemin 2014; Shaw 2006). Attempts to observe glycine in the ISM have been reported (Brown et al. 1979; Kuan et al. 2003) but its detection has never been confirmed (Snyder et al. 2005). Many theoretical studies have been devoted to proposing potential mechanisms of glycine formation in the medium (Largo et al. 2010; Redondo et al. 2015; Largo et al. 2004; Basiuk & Kobayashi 2002; Basiuk 2001; Bossa et al. 2009). Some of them include the participation of amino acid precursors (Rimola et al. 2010), which are also key candidates to be present in the ISM. In laboratory or prebiotic conditions, the famous Strecker reaction (Strecker 1850, 1854), a mixture of ammonia, hydrogen cyanide and aldehyde in water, easily leads to aminoacetonitrile. Aminoacetonitrile can be transformed to glycine by hydrolysis either in basic or acidic aqueous solution (Anslow & King 1925; Wyzlic & Soloway 1992). This last reaction is currently the most widely proposed synthesis mechanism of glycine in the ISM (Aponte et al. 2017; Zhu & Ho 2004). The hydrolysis of aminoacetonitrile occurs via the formation of the glycinamide intermediate (Rimola et al. 2012; Commeyras et al. 1983) (H_2N–CH_2–$CONH_2$) which is then hydrolyzed into the amino acid glycine (see Fig. 1). Therefore, the study of the precursors and their detection in the ISM is almost as important as that of the amino acid itself, to understand the chemical processes that could lead to the formation of building blocks of life.

Rotational spectra have been successfully used to identify most of the compounds found in interstellar space (Schlemmer et al. 2015). In 2008, aminoacetonitrile was discovered in SgrB2 (Belloche et al. 2008) by means of rotational spectroscopy data (Bogey et al. 1990). Thus, if the hydrolysis of aminoacetonitrile occurs in the gas phase or the grains of the ISM, glycinamide

should also be present in the interstellar medium. The importance of glycinamide for prebiotic chemistry was the primary motivation for the present microwave investigation. The case of glycinamide is remarkable among all the prebiotic molecules as to date no experimental investigations of this vital molecule have been reported. Its conformational landscape remains unknown.
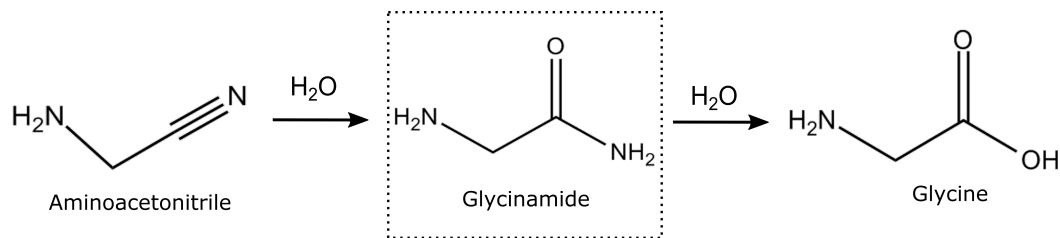

Figure 1. Hydrolysis of aminoacetonitrile in glycine via the glycinamide.

In the pure form, solid glycinamide is chemically quite unstable, reacting when exposed to the air or when heated to be vaporized, thus preventing its easy measurement in the gas phase. It is only commercially available as a hydrochloride salt, where it appears in the protonated form. At the University of Valladolid, efficient procedures have been developed for the generation of neutral forms of proteogenic amino acids in supersonic expansion by laser ablation of their zwitterionic forms, allowing their conformational investigation using Fourier transform microwave techniques (Alonso & López 2015). Very recently, a comprehensive analysis of the millimeter and submillimeter-wave spectra of aminoacetonitrile (Kolesniková et al. 2017) and laser-ablated microwave spectra of hydantoin (Alonso et al. 2017), also a potential glycine precursor, have been reported. The microwave spectrum of glycinamide, successfully generated in the gas phase by laser ablation of its hydrochloride salt, is now first reported in the present work. The precise spectroscopic information provided here could be relevant to check the existence of glycinamide in the interstellar medium.

2. EXPERIMENTAL DETAILS

In the experimental procedure, finely powdered commercial hydrochloride glycinamide sample was mixed with a small amount of a binder and pressed into cylindrical rods which were ablated using the third harmonic (355 nm) of a picosecond laser. The vaporized products were seeded in neon at backing pressures of 10-12 bar and expanded adiabatically into the vacuum chamber of the spectrometer where the glycinamide molecules liberated from the salt were probed by laser ablation broadband chirped pulse Fourier transform microwave spectroscopy (LA-CP-FTMW) (Mata et al. 2012). A high-power excitation pulse of 300 W was used to polarize the molecules at frequencies from 6 to 16 GHz. Up to 40000 individual free induction decays at a 2 Hz repetition rate were averaged in the time domain, and Fourier transformed to obtain the broadband frequency domain spectrum shown in Fig. 2.

Table 1. Observed centres of frequency and residuals (in MHz) for the rotational transitions of conformer I of glycinamide.

J'	K'_a	K'_c	J''	K''_a	K''_c	ν_{obs}	$\nu_{obs} - \nu_{calc}$
1	0	1	0	0	0	6912.185	-0.042
2	0	2	1	0	1	13688.501	0.066
1	1	0	1	0	1	6706.186	0.082
2	1	1	2	0	2	7903.277	-0.051
3	1	2	3	0	3	9933.778	-0.040
2	0	2	1	1	1	8043.501	-0.034
4	1	3	4	1	4	10535.716	-0.011
3	1	2	3	1	3	6356.274	0.055
2	1	2	1	1	1	12763.220	-0.031
2	1	1	1	1	0	14885.629	-0.030
3	0	3	2	1	2	15487.127	0.034

NOTE - ν_{obs} is the observed frequency and $\nu_{obs} - \nu_{calc}$ is the residual.
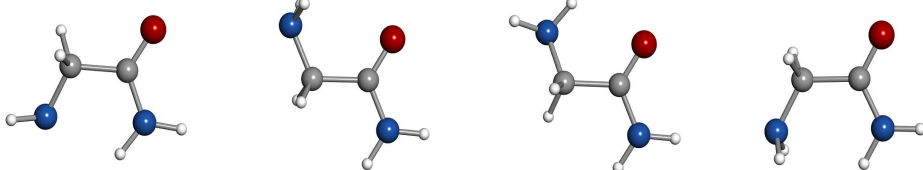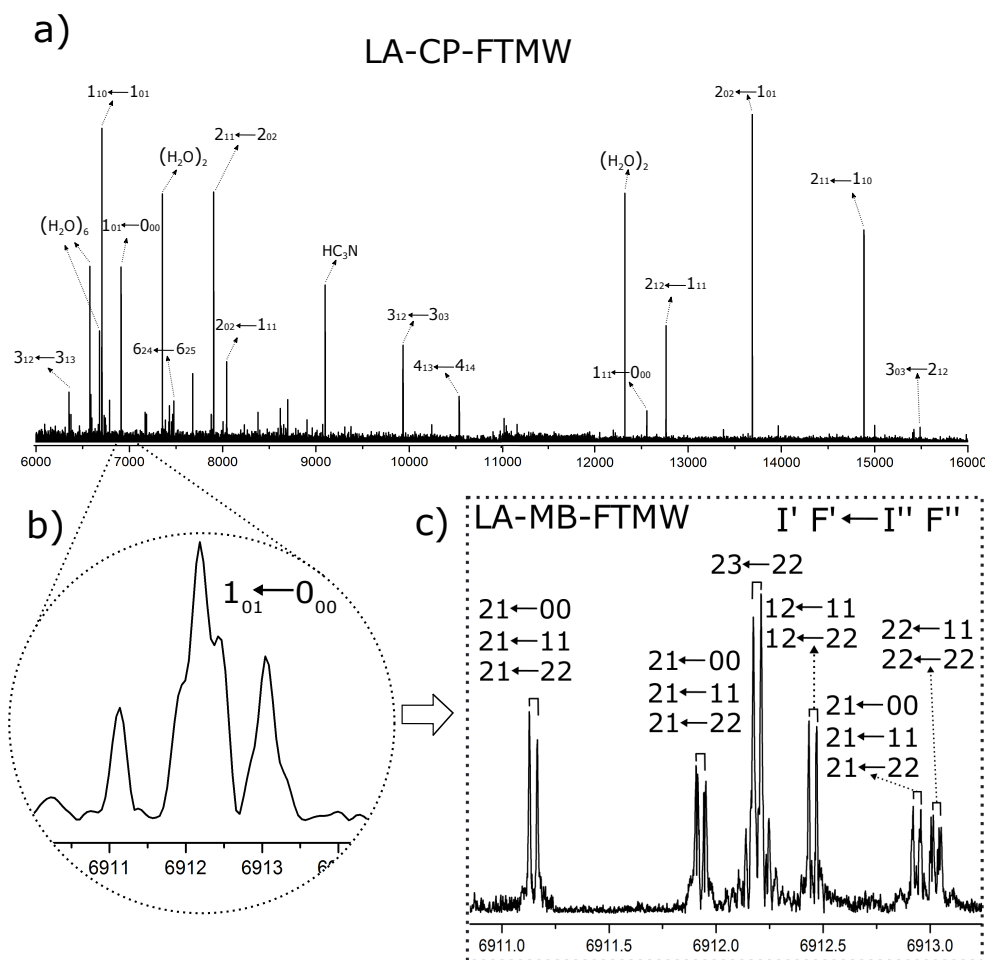
Figure 2. (a) Broadband LA-CP-FTMW spectrum of glycinamide I from 6 to 16 GHz. (b) A small section of the spectrum showing the unresolved hyperfine structure of the $1_{01} \leftarrow 0_{00}$ transition. (c) Completely resolved nuclear hyperfine structure of the $1_{01} \leftarrow 0_{00}$ transition by LA-MB-FTMW. Each hyperfine component is labeled with the corresponding values of I', F', I'', F'' quantum numbers.

3. ANALYSIS AND RESULTS

The rotational spectrum of one rotamer was easily identified due to the very intense $1_{01} \leftarrow 0_{00}$, $2_{12} \leftarrow 1_{11}$, $2_{02} \leftarrow 1_{01}$ and $2_{11} \leftarrow 1_{10}$ μ_a-type R-branch transitions. Intense μ_b-type Q-branch and weaker μ_b-type R-branch transitions were also identified. No signals belonging to other species remained unidentified in the rotational spectra apart from known lines of common decomposition products (cyanoacetylene) and of water complexes. All rotational transitions of glycinamide were observed split into complicated hyperfine patterns, with many components spanning several MHz as depicted in Fig. 2b for the $1_{01} \leftarrow 0_{00}$ transition. These complex hyperne patterns were accounted for in terms of nuclear quadrupole coupling interaction effects due to the presence in glycinamide of two ^{14}N nuclei with non-zero electric quadrupole moment and spin ($I = 1$), which interact with the electric field gradient created by the rest of the molecule at these nuclei. The ^{14}N nuclear quadrupole coupling splits the rotational energy levels decreasing the overall intensity of each rotational transition and giving rise to a very complex hyperfine structure (Gordy & Cook 1984). In a first step, no attempt was made to analyze the quadrupole hyperfine structure since the hyperfine components were not fully resolved. The rotational frequencies were measured as the intensity-weighted mean of the line clusters (see Table 1). A rigid rotor analysis generates a preliminary set of values for the rotational constants $A = 9631.61$ MHz, $B = 3986.72$ MHz, $C = 2925.51$ MHz that allows the identication of the observed rotamer of glycinamide. With this aim, a conformational search was carried out on all plausible configurations of glycinamide. Once a set of candidate structures was identified by force field and semi-empirical methods, we then employed higher-level calculations using the B3LYP density functional with the Grimme D3 dispersion interactions and Pople's 6-311++G (d,p) basis set, in order to optimize the four

Table 2. Spectroscopic parameters and relative energies calculated at the B3LYP/6-311++G(d,p) level of theory for the lowest energy conformers of glycinamide.

Parameter	I	II	III	IV
$A/B/C$	9641/3976/2925	10066/3835/2867	9952/3939/2944	9515/3894/2855
P_c	6.7	5.7	7.4	5.9
$|\mu_a|/|\mu_b|/|\mu_c|$	3.8/1.5/0.0	1.9/2.8/0.0	1.0/3.5/1.0	2.3/3.5/0.0
$^{14}N_t \, \chi_{aa}/\chi_{bb}/\chi_{cc}$	2.40/-3.66/1.26	-1.48/-0.52/2.00	2.95/2.04/-5.00	-1.50/-0.91/2.41
$^{14}N_a \, \chi_{aa}/\chi_{bb}/\chi_{cc}$	1.79/2.19/-3.99	2.32/2.31/-4.62	2.13/2.18/-4.32	2.13/2.18/-4.32
$\Delta E/ \Delta G$	0/0	745/257	1096/866	1162/934

NOTE - A, B, and C represent the rotational constants (in MHz); P_c is the planar inertial moment (in $u\text{Å}^2$), conversion factor: 505379.1 MHz-$u\text{Å}^2$; μ_a, μ_b and μ_c are the electric dipole moment components (in D); χ_{aa}, χ_{bb} and χ_{cc} are the diagonal elements of the ^{14}N nuclear quadrupole coupling tensor (in MHz), N_t and N_a correspond to the terminal and amide ^{14}N nuclei, respectively; ΔE and ΔG are the relative and Gibbs energies (in cm^{-1}) at 298 K with respect to the global minimum calculated at the B3LYP/6-311++G(d,p) with Grimme dispersion level of theory.

different structures below 1000 cm^{-1}. The predicted spectroscopic constants are collected in Table 2. The values of the rotational constants A, B, and C, which critically depend on the mass distribution, are usually a precise tool in the identication of conformers. The values predicted for the global minimum (conformer I) in Table 2 are very close to those experimentally determined.

The presence of ^{14}N nuclei in our molecule is also a helpful tool to identify structures. In our predictions, we also included the values of the quadrupole coupling constants for both $^{14}N_t$ (amine) and $^{14}N_a$ (amide) nuclei. The rotational constants give us information of the mass distribution, while the nuclear quadrupole coupling interactions have a strongly dependence on the electronic environment, position and orientation of the ^{14}N nuclei. The ^{14}N nuclei introduce hyperfine rotational probes at defined sites of glycinamide and act as a probe of the chemical environment of the N_t and N_a quadrupolar nuclei. The distinct orientation of the terminal amino group in all the conformers causes a significant effect on the values of the quadrupole coupling constants for the $^{14}N_t$ (see Table 2). To unveil, conclusively, the observed species, the treatment and interpretation of the quadrupole hyperfine structure of glycinamide is needed.

At this point we took advantage of the sub-Doppler resolution of our LA-MB-FTMW spectrometer (Alonso et al. 2009; Bermúdez et al. 2014) to fully resolve the nuclear quadrupole hyperfine structure. The analysis began with the measurement of a total of fifteen hyperfine components by interpreting the quadrupole coupling pattern for the $1_{01} \leftarrow 0_{00}$ rotational transition. Then, new predictions were carried out to finally assign a total of 63 hyperfine components (see Table 3) corresponding to four a- and two b-type transitions. Watsons A-reduced semirigid rotor Hamiltonians in the I^r-representation (Watson 1977) complemented with a term to account for the nuclear quadrupole coupling contribution (Foley 1947; Robinson & Cornwell 1953) was used for the analysis of the transitions. The quadrupole coupling Hamiltonian was set up in the coupled basis set ($I_1 I_2 I J K F$), where $I_1 + I_2 = I$, $I + J = F$. The energy levels involved in each transition are thus labeled with the quantum numbers J, K_a, K_c, I, F. Table 4 reports accurate rotational and nuclear quadrupole constants determined from such analysis. Thus, a final comparison between the experimental and theoretical values of spectroscopic constants allows the unambiguous identication of the observed rotamer as conformer I.

4. DISCUSSION AND CONCLUSION

An unexpected observation from the results of Table 4 is the abnormal non-rigid behavior reflected in the large values of the centrifugal distortion constants Δ_{JK} and Δ_K despite the low J values of the rotational energy levels involved in the measured transitions. This fact is confirmed by the comparison of the rms deviations from the rigid and semirigid rotor analysis in Table 3. The origin of the non-rigid behavior can be attributed to the existence of a large amplitude C_2–N_t bond torsion controlled by a double minimum potential function with a low energy barrier to the planar configuration. For such potential functions, the vibrational energy levels occur at energy intervals comparable in magnitude to those of the rotational levels. Coriolis coupling

Table 3. Observed frequencies and residuals with or without centrifugal distortional constants (in MHz) for the rotational transitions of conformer I of glycinamide.

| J'	K'_a	K'_c	I'	F'	J''	K''_a	K''_c	I'	F'	ν_{obs}	$\nu_{obs}-\nu_{calc}$ with distortion	$\nu_{obs}-\nu_{calc}$ without distortion	J'	K'_a	K'_c	I'	F'	J''	K''_a	K''_c	I'	F'	ν_{obs}	$\nu_{obs}-\nu_{calc}$ with distortion	$\nu_{obs}-\nu_{calc}$ without distortion
1	1	1	1	1	0	0	0	0	0	12555.898	-0.003	-0.004	1	1	0	2	2	1	0	1	2	3	6705.377	-0.001	0.006
1	1	1	1	1	0	0	0	1	1	12555.898	-0.003	-0.004	1	1	0	2	3	1	0	1	2	2	6705.539	0.002	0.003
1	1	1	1	1	0	0	0	2	2	12555.898	-0.003	-0.004	1	1	0	1	1	1	0	1	2	1	6706.205	0.001	0.018
1	1	1	2	2	0	0	0	1	1	12556.447	-0.001	-0.004	1	1	0	1	2	1	0	1	1	2	6706.339	-0.006	0.008
1	1	1	2	2	0	0	0	2	2	12556.447	-0.001	-0.004	1	1	0	2	3	1	0	1	2	3	6706.374	0.002	0.004
1	1	1	1	0	0	0	0	1	1	12556.938	-0.001	-0.006	1	1	0	2	2	1	0	1	2	1	6706.421	0.002	0.012
1	1	1	0	1	0	0	0	0	0	12557.231	0.000	-0.005	2	0	2	0	2	1	0	1	0	1	13687.508	-0.001	0.021
1	1	1	0	1	0	0	0	1	1	12557.231	0.000	-0.005	2	0	2	2	1	1	0	1	2	2	13687.571	-0.002	0.020
1	1	1	0	1	0	0	0	2	2	12557.231	0.000	-0.005	2	0	2	2	1	1	0	1	0	1	13687.660	0.001	0.022
1	1	1	2	3	0	0	0	2	2	12557.284	-0.001	-0.006	2	0	2	1	2	1	0	1	0	1	13687.660	0.001	0.022
1	1	1	1	2	0	0	0	1	1	12557.774	-0.002	-0.009	2	0	2	1	2	1	0	1	1	2	13688.147	-0.001	0.021
1	1	1	1	2	0	0	0	2	2	12557.774	-0.002	-0.009	2	0	2	1	1	1	0	1	1	0	13688.246	-0.003	0.018
1	1	1	2	1	0	0	0	0	0	12558.891	-0.003	-0.012	2	0	2	2	4	1	0	1	2	3	13688.610	-0.001	0.021
1	1	1	2	1	0	0	0	1	1	12558.891	-0.003	-0.012	2	0	2	1	3	1	0	1	1	2	13688.742	0.000	0.024
1	1	1	2	1	0	0	0	2	2	12558.891	-0.003	-0.012	2	0	2	0	2	1	0	1	2	1	13689.303	0.001	0.027
1	0	1	2	1	0	0	0	0	0	6911.146	0.003	0.026	2	0	2	2	3	1	0	1	2	3	13689.422	0.005	0.027
1	0	1	2	1	0	0	0	1	1	6911.146	0.003	0.026	2	0	2	1	1	1	0	1	1	1	13689.609	0.000	0.020
1	0	1	2	1	0	0	0	2	2	6911.146	0.003	0.026	2	1	1	2	0	1	1	0	2	1	14883.765	0.000	0.005
1	0	1	1	1	0	0	0	0	0	6911.924	-0.001	0.026	2	1	1	2	1	1	1	0	1	2	14884.366	-0.001	0.007
1	0	1	1	1	0	0	0	1	1	6911.924	-0.001	0.026	2	1	1	1	2	1	1	0	1	2	14884.681	0.001	-0.010
1	0	1	1	1	0	0	0	2	2	6911.924	-0.001	0.026	2	1	1	2	1	1	1	0	0	1	14884.681	0.001	-0.010
1	0	1	2	3	0	0	0	2	2	6912.191	0.006	0.032	2	1	1	2	2	1	1	0	2	1	14884.777	0.000	-0.006
1	0	1	1	2	0	0	0	1	1	6912.453	0.002	0.027	2	1	1	1	1	1	1	0	2	1	14885.160	-0.001	-0.009
1	0	1	1	2	0	0	0	2	2	6912.453	0.002	0.027	2	1	1	2	1	1	1	0	1	0	14885.359	-0.001	-0.013
1	0	1	0	1	0	0	0	0	0	6912.937	0.001	0.028	2	1	1	2	4	1	1	0	2	3	14885.634	0.002	-0.014
1	0	1	0	1	0	0	0	1	1	6912.937	0.001	0.028	2	1	1	0	2	1	1	0	0	1	14885.779	0.002	-0.015
1	0	1	0	1	0	0	0	2	2	6912.937	0.001	0.028	2	1	1	2	1	1	1	0	1	1	14885.810	-0.005	-0.028
1	0	1	2	2	0	0	0	1	1	6913.018	-0.002	0.026	2	1	1	1	3	1	1	0	2	2	14886.036	-0.002	-0.021
1	0	1	2	2	0	0	0	2	2	6913.018	-0.002	0.026	2	1	1	2	3	1	1	0	1	2	14886.348	-0.001	-0.014
1	0	1	1	0	0	0	0	1	1	6913.289	0.004	0.031	2	1	2	2	4	1	1	1	2	3	12763.202	0.008	-0.075
1	1	0	1	2	1	0	1	0	1	6705.868	0.008	0.004	2	1	2	1	3	1	1	1	2	2	12763.736	-0.002	-0.080
1	1	0	1	0	1	0	1	1	1	6705.879	0.002	0.002	..	...	...	...	...	...	...	...	...	...	...	...	...

NOTE - ν_{obs} is the observed frequency and $\nu_{obs}-\nu_{calc}$ is the residual.

interactions can, in such situation, take place between the observed ground vibrational state with the first torsional excited state, but the latter is not-observed since it is expected to be depopulated due to vibrational cooling. When these interactions are small, they can be treated as perturbations, and their effects are reflected in abnormally high centrifugal distortion constants. In order to confirm the presence of such a double minimum potential we varied the amine ∠CCNH dihedral angle and the calculations point to such a double minimum potential separated by a barrier of 116 cm^{-1} (see Fig. 3). As can be seen, this torsion barrier connects the two isoenergetic conformers and it is sufficiently low to allow Coriolis coupling rationalizing the need to use sizable centrifugal distortional constants at low J values.

The first experimental information on the conformational properties of glycinamide is presented in this study. The capability provided by the laser ablation coupled with time domain Fourier transform microwave techniques to obtain very accurate spectroscopic constants, that in combination with theoretical computations, enables the unequivocal identification of the observed species. The two ^{14}N$_t$ and ^{14}N$_a$ nuclei of glycinamide act as hyperfine rotational probes of molecular conformation that enlarge even more the usefulness of this spectroscopic technique. The obtained results indicate that glycinamide exits in the gas phase in a single conformation, stabilized by a N$_a$–H $\cdots$ N$_t$H$_2$ hydrogen bond, which is the geometry predicted as the global minimum. The experimental approach followed in this study is an unique tool to pave the way towards more complex, unstable systems

Table 4. Experimental spectroscopic constants of the observed conformer I of glycinamide.

Parameter	Rigid rotor analysis	Semirigid rotor analysis
A	9631.6462 (65)	9631.998 (33)
B	3986.7564 (34)	3986.78631 (82)
C	2925.5858 (37)	2925.58244 (58)
Δ_{JK}	...	-0.02554 (62)
Δ_{K}	...	-0.302 (32)
χ_{aa} (N_t)	2.097 (23)	2.1121 (57)
χ_{bb} (N_t)	-3.121 (23)	-3.1135 (15)
χ_{cc} (N_t)	1.024 (23)	1.0014 (15)
χ_{aa} (N_a)	1.567 (26)	1.5547 (32)
χ_{bb} (N_a)	1.968 (30)	1.9597 (38)
χ_{cc} (N_a)	-3.535 (30)	-3.5145 (38)
σ	23.9	2.8
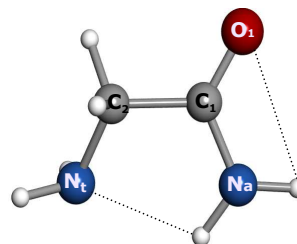
NOTE - A, B, and C are the rotational constants (in MHz); Δ_{JK} and Δ_K are the quartic centrifugal distortion constants (in MHz); χ_{aa}, χ_{bb} and χ_{cc} are the diagonal elements of the ^{14}N nuclear quadrupole coupling tensor (in MHz), N_t and N_a correspond to the amino ^{14}N and amide ^{14}N nuclei, respectively; σ is the root mean square deviation of the fit (in kHz).
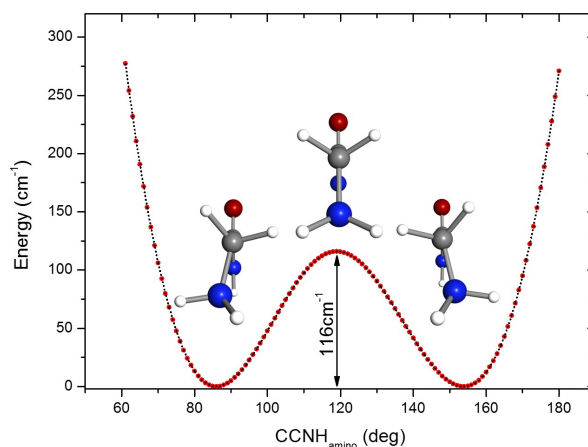

Figure 3. Potential energy surface scan of the CCNH amino torsion as a function of the energy. A barrier of 116 cm^{-1} interconnects the two iso-energetic conformers.

which have been discarded until now because of being considered out of reach of high-resolution spectroscopic studies. This is the case of many molecules, like glycinamide, considered potential candidates to be present in the ISM. The spectroscopic constants presented in this work constitute a first step to identify this glycine precursor in the ISM. Also, for observations in low frequency regions like the ones accessible for the Green Bank Telescope, the hyperfine components of the transitions, which normally are propagated several MHz, could result to be a handicap for interpreting the radioastronomical observations. In this work, the experimental values of the ^{14}N nuclear quadrupole coupling constants are also provided in order to reproduce perfectly the spectrum to enable its distinct possible identification.

REFERENCES

Alonso, E. R., Kolesniková, L., & Alonso, J. L. 2017, JChPh, 147, 124312

Alonso, J. L., & López, J. C. 2015, Microwave Spectroscopy of Biomolecular Building Blocks, ed. A. M. Rijs & J. Oomens (Cham: Springer International Publishing), 335–401

Alonso, J. L., Perez, C., Eugenia Sanz, M., Lopez, J. C., & Blanco, S. 2009, PCCP, 11, 617

Anslow, W. K., & King, H. 1925, Org. Synth., 4, 31

Aponte, J. C., Elsila, J. E., Glavin, D. P., et al. 2017, ACS Earth and Space Chemistry, 1, 3

Basiuk, V. A. 2001, JPCA, 105, 4252

Basiuk, V. A., & Kobayashi, K. 2002, Viva Origino, 30, 54

Belloche, A., Menten, K. M., Comito, C., et al. 2008, A&A, 482, 179

Bermúdez, C., Mata, S., Cabezas, C., & Alonso, J. L. 2014, Angew. Chem. Int. Ed., 53, 11015

Bogey, M., Dubus, H., & Guillemin, J. 1990, JMoSp, 143, 180

Bossa, J.-B., Duvernay, F., Theulé, P., et al. 2009, A&A, 506, 601

Brown, R. D., Godfrey, P. D., Storey, J. W. V., et al. 1979, MNRAS, 186, 5P

Commeyras, A., Taillades, J., Brugidou, J., et al. 1983, Eur. Pat. Appl., EP 84470 A1 19830727

Foley, H. M. 1947, PhRv., 71, 747

Gordy, W., & Cook, R. 1984, Microwave molecular spectra, Techniques of chemistry (Wiley)

Guillemin, J.-C. 2014, BIO Web of Conferences, 2, 04002

Kolesniková, L., Alonso, E. R., Mata, S., & Alonso, J. L. 2017, ApJS, 229, 26

Kuan, Y.-J., Charnley, S. B., Huang, H.-C., Tseng, W.-L., & Kisiel, Z. 2003, ApJ, 593, 848

Kwok, S., ed. 2011, Organic Matter in the Universe (Wiley-Blackwell)

Largo, A., Redondo, P., & Barrientos, C. 2004, IJQC, 98, 355

Largo, L., Barrientos, C., Rayón, V. M., Largo, A., & Redondo, P. 2010, IJMSp, 295, 21

Mata, S., Pena, I., Cabezas, C., López, J., & Alonso, J. 2012, JMoSp, 280, 91

Redondo, P., Largo, A., & Barrientos, C. 2015, A&A, 579, A125

Rimola, A., Sodupe, M., & Ugliengo, P. 2010, PCCP, 12, 5285

—. 2012, ApJ, 754, 24

Robinson, G. W., & Cornwell, C. D. 1953, JChPh, 21, 1436

Schlemmer, S., Giesen, T., & Mutschke, H., eds. 2015, Laboratory Astrochemistry: From Molecules through Nanoparticles to Grains (Wiley-Blackwell)

Shaw, A. M. 2006, Astrochemistry: From Astronomy to Astrobiology (Wiley-Blackwell)

Snyder, L. E., Lovas, F. J., Hollis, J. M., et al. 2005, ApJ, 619, 914

Strecker, A. 1850, Justus Liebigs Annalen der Chemie, 75, 27

—. 1854, Justus Liebigs Annalen der Chemie, 91, 349

Watson, J. K. G. 1977, in Vibrational Spectra and Structure, ed. J. R. Durig, Vol. 6 (Amsterdam: Elsevier), 1–89

Wyzlic, I. M., & Soloway, A. H. 1992, Tetrahedron Lett., 33, 7489

Zhu, H.-S., & Ho, J.-J. 2004, JPCA, 108, 3798